Molecules and Cells

The Aurora Kinase Inhibitor CYC116 Promotes the Maturation of Cardiomyocytes Derived from Human Pluripotent Stem Cells

Sijia Ji[1,2,3], Wanzhi Tu[1,2,3], Chenwen Huang[2], Ziyang Chen[2,3], Xinyue Ren[2,3], Bingqing He[1,2,3], Xiaoyan Ding[4], Yuelei Chen[4], and Xin Xie[1,2,3,5,*]

[1]School of Life Science and Technology, ShanghaiTech University, Shanghai 201210, China, [2]State Key Laboratory of Drug Research, The National Center for Drug Screening, Shanghai Institute of Materia Medica, Chinese Academy of Sciences, Shanghai 201203, China, [3]University of Chinese Academy of Sciences, Beijing 100049, China, [4]Stem Cell Bank/Stem Cell Core Facility, Institute of Biochemistry and Cell Biology, Chinese Academy of Sciences, Shanghai 200031, China, [5]School of Pharmaceutical Science and Technology, Hangzhou Institute for Advanced Study, University of Chinese Academy of Sciences, Hangzhou 310024, China
*Correspondence: xxie@simm.ac.cn
https://doi.org/10.14348/molcells.2022.0077
www.molcells.org

Human pluripotent stem cell-derived cardiomyocytes (hPSC-CMs) have great potential in applications such as regenerative medicine, cardiac disease modeling, and *in vitro* drug evaluation. However, hPSC-CMs are immature, which limits their applications. During development, the maturation of CMs is accompanied by a decline in their proliferative capacity. This phenomenon suggests that regulating the cell cycle may facilitate the maturation of hPSC-CMs. Aurora kinases are essential kinases that regulate the cell cycle, the role of which is not well studied in hPSC-CM maturation. Here, we demonstrate that CYC116, an inhibitor of Aurora kinases, significantly promotes the maturation of CMs derived from both human embryonic stem cells (H1 and H9) and iPSCs (induced PSCs) (UC013), resulting in increased expression of genes related to cardiomyocyte function, better organization of the sarcomere, increased sarcomere length, increased number of mitochondria, and enhanced physiological function of the cells. In addition, a number of other Aurora kinase inhibitors have also been found to promote the maturation of hPSC-CMs. Our data suggest that blocking aurora kinase activity and regulating cell cycle progression may promote the maturation of hPSC-CMs.

Keywords: Aurora kinase inhibitor, cardiomyocyte differentiation, cell cycle, human pluripotent stem cell, maturation

INTRODUCTION

Human pluripotent stem cells (hPSCs), including embryonic stem cells (ESCs) and induced pluripotent stem cells (iPSCs), have been successfully differentiated into cardiomyocytes (CMs) *in vitro*. Cardiomyocytes derived from human pluripotent stem cells (hPSC-CMs) have many potential applications, especially in heart disease-related regeneration therapy and in exploring the mechanism of hereditary heart diseases (Moretti et al., 2010; Yang et al., 2014). hPSC-CMs can also be used to screen new drugs and evaluate the cardiac toxicology of investigational new drugs *in vitro* (Liang et al., 2013; Tertoolen et al., 2018). Although cardiomyocytes derived from traditional two-dimensional (2D) differentiation methods have many similarities with human primary cardiomyocytes in terms of molecular, structural and functional characteristics, they are still in the immature fetal stage (around 20 weeks of gestation) (Cao et al., 2008; Xu et al., 2009), and they

Received 6 May, 2022; revised 18 September, 2022; accepted 20 September, 2022; published online 13 December, 2022

eISSN: 0219-1032

differ significantly from adult CMs in both morphology and function, which severely limits the application of hPSC-CMs (Robertson et al., 2013).

To solve this key problem, researchers have proposed different methods to promote the maturation of hPSC-CMs. Apart from prolonged (up to 1 year) culture under 2D culture conditions (Kamakura et al., 2013), three-dimensional (3D) cultures in various substrates have also been reported to facilitate the maturation of hPSC-CMs (Kadota et al., 2017; Mills et al., 2017; Ronaldson-Bouchard et al., 2018). As an alternative to complicated 3D conditions, biochemical stimulation with various small molecules has also been reported to promote the maturation of hPSC-CMs in 2D cultures. Triiodothyronine (T3) and dexamethasone have been found to improve the sarcomere length, mitochondrial functions and excitation-contraction coupling of hPSC-CMs when used alone or in combination (Parikh et al., 2017; Yang et al., 2014). Replacing glucose in the medium with free fatty acids also improves the mitochondrial content, functional gene expression, sarcomere length and contractility of hPSC-CMs by changing the metabolic mode of these cells (Hu et al., 2018; Yang et al., 2019). Other compounds, including corticosterone, ZLN005, Torin 1 and retinoic acid, have also been reported to promote the maturation of hPSC-CMs in *in vitro* culture (Garbern et al., 2020; Liu et al., 2020; Miao et al., 2020; Rog-Zielinska et al., 2015).

To identify more small molecule compounds that can promote the maturation of hPSC-CMs, we established a human PSC-to-CM differentiation system and screened a series of compounds. We found that CYC116, an inhibitor of Aurora kinases, which play important roles in cell cycle regulation (Borisa and Bhatt, 2017), significantly promoted the maturation of CMs derived from both human ESCs (hESCs) (H1 and H9) and iPSCs (UC013), resulting in increased expression of genes related to cardiomyocyte function, better organization of the sarcomere, increased sarcomere length, increased number of mitochondria, and enhanced physiological function of the cells. In addition, a number of other Aurora kinase inhibitors, including Aurora A/B inhibitors (VX-680 and SNS-314), Aurora A inhibitors (MLN8237 and MK8745), and Aurora B inhibitors (GSK1070916 and Barasertib), were also found to promote the maturation of hPSC-CMs, indicating that the regulation of the cell cycle can effectively promote the maturation of hPSC-CMs and pave the way for the large-scale acquisition of relatively mature cardiomyocytes.

MATERIALS AND METHODS

hPSC culture and differentiation

The hESC lines H1 and H9 were obtained from WiCell Research Institute (USA). UC013 is a human iPSC (hiPSC) cell line reprogrammed from the urine cells of a 28-year-old male by Duanqing Pei's lab (Xue et al., 2013) from Guangzhou Institute of Biomedicine and Health, Chinese Academy of Sciences (China). Experiments in this study were approved and conducted in accordance with the guidelines of the Institutional Review Board of Shanghai Institute of Materia Medica (approval No. SIMMEC2022004). hPSCs were cultured in feeder-free conditions on Matrigel-coated plates (BD Biosciences, USA) and fed mTeSR1 medium (STEMCELL Technologies, Canada). The method for hPSC to CM differentiation was adapted from previous publications (Bhattacharya et al., 2014; Burridge et al., 2014) and is summarized in Supplementary Fig. S1A. Briefly, on Day -2, hPSCs were dissociated into single cells with Versene (Gibco, USA) and replated at a density of 300,000 cells per well on 12-well plates in mTeSR1 with 10 μM Y-27632 (MedChemExpress, USA). On Day -1, the cells received fresh mTeSR1 without Y-27632. To induce cardiogenesis, the medium was changed to differentiation medium consisting of RPMI 1640 (Gibco) and 2% B27 minus insulin (Gibco). For Days 0-2, the differentiation medium was supplemented with 6 μM CHIR99021 (MedChemExpress). On Day 2, the medium was changed to fresh differentiation medium. For Days 3-5, the differentiation medium was supplemented with 2 μM IWR-1 (MedChemExpress). The differentiation medium was changed on Day 5 and every other day thereafter. Beating cells (hPSC-CMs) could be observed beginning on Day 7. To test the efficacy of CYC116 in promoting the maturation of hPSC-CMs, cells were dissociated with Accutase (STEMCELL Technologies) and replated at a density of 400,000 cells per well on 12-well plates in maintenance medium consisting of RPMI 1640 and 2% B27 (Gibco) on Day 12. After 48 h, compounds were added to the maintenance medium for various durations. The medium was changed every other day.

Flow cytometry analysis

hPSC-CMs were dissociated with Accutase and washed with phosphate-buffered saline (PBS). Cells were then fixed in 4% paraformaldehyde (PFA) for 10 min, permeabilized with 0.1% Triton X-100 for 10 min and incubated with 1:200 mouse anti-cTnt (Invitrogen, USA) at 4°C overnight. Secondary staining was performed with a secondary antibody conjugated to Alexa Fluor 488 (1:1,000; Molecular Probes, USA) for 1 h at room temperature. Samples were analyzed with an ACEA NovoCyte flow cytometer.

Quantitative real-time polymerase chain reaction (qRT-PCR) analysis

Total mRNA was isolated using TRIzol (Invitrogen), and 1 μg mRNA was used to synthesize cDNA using the PrimeScript RT Master Mix reagent kit (Takara, Japan) according to the manufacturer's protocol. Real-time PCR was performed using 2× SYBR Green qPCR Master Mix (Biotool, USA) and a Stratagene Mx 3000P thermal cycler. Samples were normalized using *GAPDH* as a housekeeping gene. To measure the mtDNA content, total DNA was extracted using a TIANamp Genomic DNA Kit (DP304-03; Tiangen Biotech, China). The content of mtDNA (*ND1*, *ND2*, *ND4*, *ND5*, *ND6*, *Cox1*, *Cox2*, *Cox3*, *ATP6*, *D-loop*, *RNR2*, etc.) was normalized to nDNA encoding *β-globin* in the same sample. The sequences of the primers are listed in Supplementary Table S1.

Immunofluorescent staining

On Day 30, hPSC-CMs were dissociated with accutase and replated at a density of 50,000 cells per well on a 24-well plate coated with Matrigel in maintenance medium. To reveal the sarcomere structure and cell area, cells were fixed

with 4% PFA and permeabilized with 0.3% Triton X-100. After blocking with 5% bovine serum albumin for 30 min, the cells were incubated with mouse anti-α-Actinin (1:1,000; Sigma-Aldrich, USA) or mouse anti-cTnt (1:200; Invitrogen) at 4°C overnight. After thorough washing, the cells were stained with secondary antibody conjugated with Alexa Fluor 555 (1:1,000; Molecular Probes) for 1 h at room temperature. Nuclei were counterstained with Hoechst 33342 (Sigma-Aldrich). Images were captured with an Olympus FV10i confocal microscope. The sarcomere length and cell area were analyzed using ImageJ software.

Transmission electron microscopy (TEM)

hPSC-CMs were detached by accutase and centrifuged into pellets. The cell pellet was washed in PBS 3 times and fixed with 2.5% glutaraldehyde for 2 h. Then, the pellet was washed, fixed in 1% osmium tetroxide, dehydrated in acetone and embedded in epoxy resin (EPON). Then, 70 nm thin sections were cut with a diamond knife, mounted on copper slot grids coated with Formvar and stained with uranyl acetate and lead citrate for examination on a Talos L120C transmission electron microscope at 120 kV.

Patch-clamp recording

On Day 30, hPSC-CMs were dissociated with accutase and replated at a density of 100,000 cells per well on a 24-well plate with glass cover slips coated with Matrigel. Patch-clamp recording was performed in a temperature-controlled room at approximately 25°C. The Giga-Ohm seal was achieved under voltage-clamp mode, and the action potentials (APs) were recorded under the current-clamp configuration using a Multiclamp 700B (Axon, USA). The pipette solution contained 140 mM KCl, 1 mM $MgCl_2$, 10 mM EGTA, and 10 mM HEPES (pH 7.2 with KOH). During the recording, constant perfusion of extracellular solution was maintained using a BPS perfusion system (ALA Scientific Instruments, USA). The extracellular solution contained 140 mM NaCl, 5 mM KCl, 1 mM $CaCl_2$, 1.25 mM $MgCl_2$, 10 mM HEPES and 10 mM glucose (pH 7.4 with NaOH). Signals were filtered at 1 kHz and digitized using DigiData 1440 with pClamp9.2 software (Molecular Devices, USA).

Intracellular Ca^{2+} measurement

To record calcium transients, the hPSC-CMs were incubated with 2 μM Fluo-4 AM in cell culture medium at 37°C for 30 min. After removing excess dye in the medium, spontaneous Ca^{2+} transients were recorded at 37°C using a high-resolution living cell imaging system (GE Healthcare, USA). The recording lasted for at least 30 seconds for each field. The peak time and decay time of each beat were recorded and analyzed with Prism 8.0.1 (GraphPad Software, USA).

Propidium iodide (PI) staining

To detect the ploidy changes in hPSC-CMs, PI staining was performed, and the changes in cell ploidy were detected by flow cytometry. On Day 30, hPSC-CMs were dissociated with accutase, washed with PBS once, and then soaked in eBioscience™ fixation & permeabilization buffer for 20 min at 4°C. After washing three times, the cells were incubated at 4°C in PBS containing 10 μg/ml PI dye and 200 μg/ml RNase for 15 min. Then, the samples were incubated with PBS containing only 200 μg/ml RNase as a negative control. Samples were analyzed with an ACEA NovoCyte flow cytometer.

Oxygen consumption assay

On Day 30, hPSC-CMs were dissociated with accutase and replated at a density of 5,000 cells per well on a Seahorse XF96 cell culture microplate (Seahorse Bioscience, USA). Oxygen consumption rates (OCRs) of differentiated cells were measured in a Seahorse XF96 Analyzer (Seahorse Bioscience) according to the manufacturer's protocol. OCRs were measured under basal conditions and after the addition of oligomycin (2 μM), carbonyl cyanide 4-(trifluoromethoxy) phenylhydrazone (FCCP, 1 μM) and rotenone/antimycin A (1 μM).

Transcriptome analysis

Total RNA of H9-CMs induced with CYC116 or DMSO treatment was isolated and underwent commercial RNA-seq analysis (Berry Genomics, USA). In brief, a library for RNA sequencing was prepared as follows: First, total RNA was isolated using TRIzol according to the manufacturer's instructions. Second, mRNA was purified from total RNA and then reverse-transcribed to cDNA for sequencing. Finally, after library preparation and pooling of different samples, the samples were subjected to Illumina PE150 (paired-end 150 nt) sequencing. A heatmap was constructed using R software (v4.1.0; https://www.r-project.org). Gene set enrichment analysis (GSEA) was performed to identify the significantly enriched pathways of H9-CMs induced with various treatments (Online: https://www.gsea-msigdb.org/gsea/index.jsp; Software: GSEA v4 desktop).

Statistical analyses

All the data are presented as the mean ± SEM, and between-group differences were analyzed using Student's *t*-test. All comparisons were two-tailed, and $P < 0.05$ was considered statistically significant. All graphs were plotted with GraphPad Prism software.

RESULTS

The Aurora kinase inhibitor CYC116 increases the expression of cardiac-related genes in H1-derived CMs (H1-CMs)

To identify small molecule compounds that may promote the maturation of hPSC-CMs, we established an hPSC to cardiomyocyte differentiation protocol adopted from previous publications (Bhattacharya et al., 2014; Burridge et al., 2014) and screened a range of inhibitors. Among these compounds, we found that the Aurora kinase inhibitor CYC116 increased the expression of genes related to mature cardiomyocyte functions in H1-CMs. To confirm the efficacy of CYC116 in promoting the maturation of H1-CMs, a series of treatment time ranges (Scheme 1: Days 14-22, Scheme 2: Days 14-26, Scheme 3: Days 14-30, Scheme 4: Days 18-30, Scheme 5: Days 22-30) and concentrations (0.5 μM, 1.5 μM, and 5 μM) were designed (Supplementary Fig. S1A). qRT-PCR was performed on the 30th day of differentiation. The results showed that the mRNA levels of cardiac markers were most

significantly increased by 5 μM CYC116 treatment (Supplementary Fig. S1B); however, the cell number was severely reduced with a long period of 5 μM CYC116 treatment (12 days or 16 days; Supplementary Fig. S1C). Considering the efficiency and final cell number, we determined to treat cardiomyocytes with 5 μM CYC116 (Scheme 5, Days 22-30) in further experiments (Fig. 1A). Interestingly, the expression of Aurora kinases A and B kept reducing during cardiomyocyte

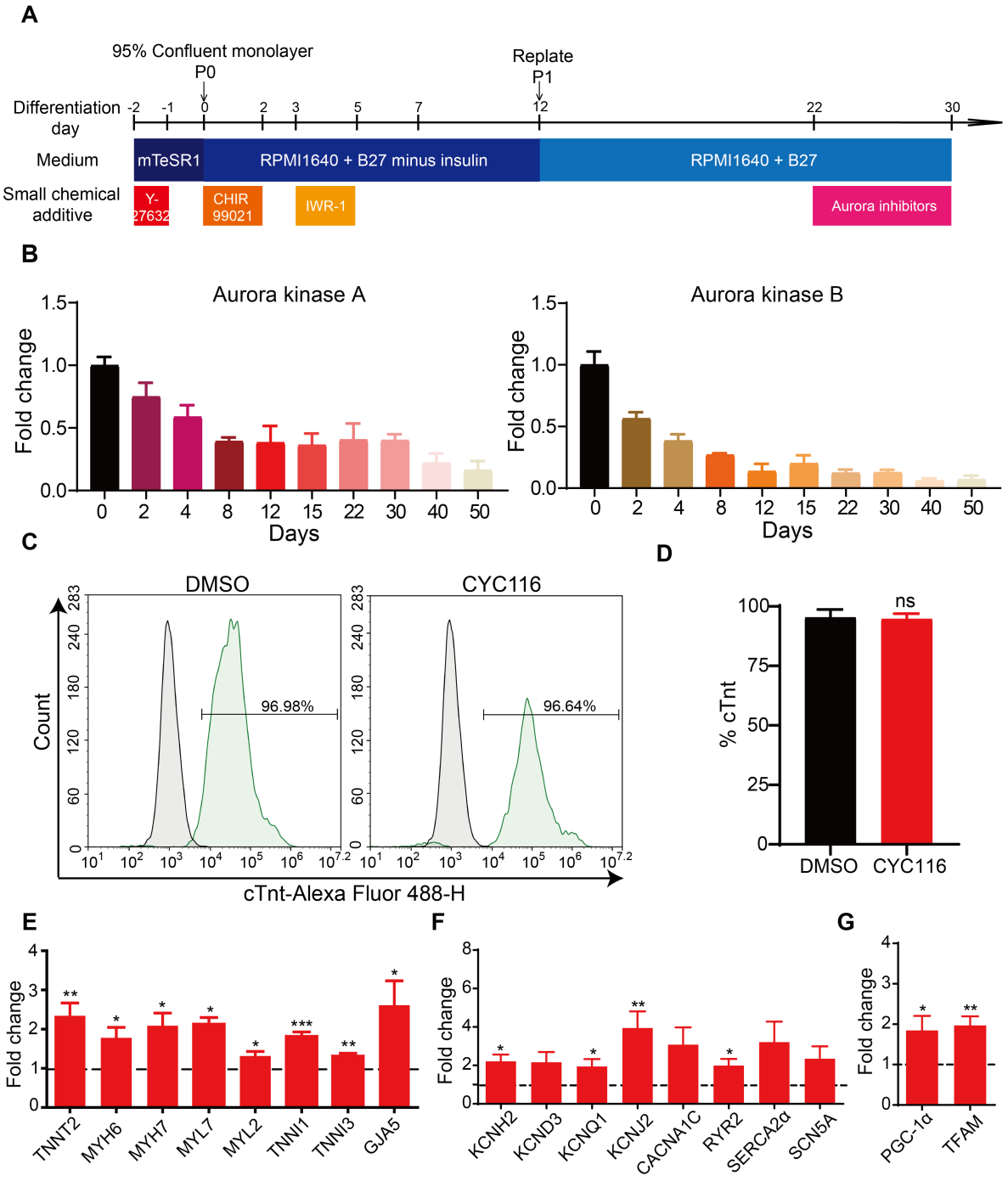

Fig. 1. CYC116 increases the expression of cardiac related genes in H1-derived cardiomyocytes (H1-CMs). (A) Schematic representation of experimental timeline and various media used for hESC-H1 culture and cardiomyocyte differentiation and maturation. (B) The expression of Aurora kinase A and Aurora kinase B were significantly decreased during cardiomyocyte differentiation (n = 3). (C and D) FACS analysis of cTnt staining in H1-CMs treated with DMSO or CYC116 (n = 3). (E-G) qRT-PCR analysis of the mRNA levels of genes related to cardiac structure (E), ion channels (F), and mitochondrial functions (G) in H1-CMs treated with DMSO (dashed line) or CYC116 (n = 3). Data are presented as mean ± SEM. $*P < 0.05$; $**P < 0.01$; $***P < 0.001$; ns, not significant.

differentiation (Fig. 1B), indicating that these kinases play a role in cell proliferation in early stages but are downregulated during differentiation and maturation. This finding also suggests that applying CYC116 at a late stage would be more beneficial.

CYC116 did not significantly increase the percentage of cTnt$^+$ cells (Figs. 1C and 1D), but CYC116 significantly increased the expression of genes related to mature cardiomyocyte functions (Figs. 1E-1G), including genes associated with sarcomere structure (*TNNT2, MYH6, TNNI1*, etc.), gap junction (*GJA5*), ion channels and transporters (*KCNH2*, *KCNQ1*, *RYR2, SERCA2α*, etc.), and energy metabolism (*PPARGC1A* and *TFAM*). These data suggest that CYC116 promotes the expression of genes related to cardiomyocyte maturation in H1-CMs without changing the differentiation efficiency.

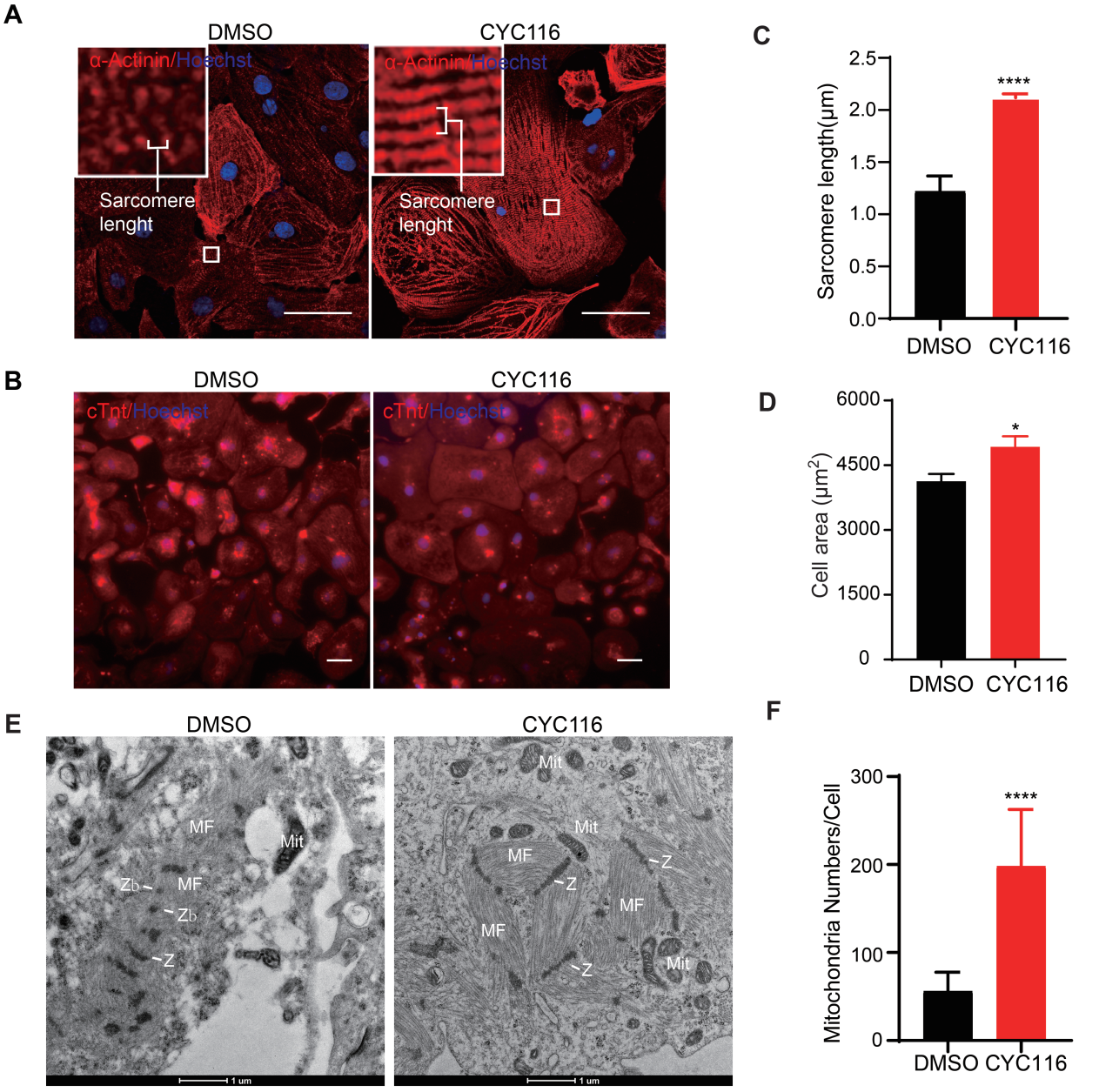

Fig. 2. CYC116 improves structural and mitochondrial maturation of H1-derived cardiomyocytes (H1-CMs). (A and B) Representative images of immunofluorescence staining of α-Actinin and cTnt in DMSO- and CYC116-treated H1-CMs. Scale bars = 50 μm. (C and D) Sarcomere length (C) and cell area (D) measured from (A) and (B), respectively. Myofibrils with at least ten well recognized, continuous α-Actinin$^+$ bands were measured and the length were divided by the number of sarcomeres. The cell area of cTnt$^+$ H1-CMs is calculated by total fluorescence intensity/cell number (C) (n = 20-30 cells). (E) Transmission electron microscopy (TEM) images of H1-CMs treated with DMSO or CYC116. MF, myofibrils; Z, Z-bands; Zb, Z-bodies; Mit, mitochondria. Scale bars = 1 μm. (F) Quantification of mitochondria per CM with TEM images (n = 25 cells). Data are presented as the mean ± SEM. $*P < 0.05$; $****P < 0.0001$.

CYC116 improves the structural and mitochondrial maturation of H1-CMs

The sarcomere is the fundamental unit for cardiomyocyte contraction. During the development of cardiomyocytes, the density of sarcomeres greatly increases, and they become longer and gradually align in order. Myofibrils fill 40% to 52% of the cytoplasmic volume in adult cardiomyocytes (Barth et al., 1992). Meanwhile, the morphology and function of mitochondria are also important indicators of cardiomyocyte maturity. During development, the number, intimal area, and cristae of mitochondria increase with the maturation of cardiomyocytes. Adult hearts show higher mitochondrial mass (occupying 15% to 25% of the cytoplasmic volume) and increased copy numbers of mitochondrial DNA (mtDNA) (Barth et al., 1992; Goffart et al., 2004). In addition, the distribution of junctional organization is an important factor that regulates conduction velocity. The adherens junction protein N-cadherin and the gap junction protein Connexin 43 are distributed circumferentially and at low density during fetal life. As the postnatal rodent heart matures, these proteins become progressively concentrated into intercalated disks at the ends of the cells, and their density increases (Angst et al., 1997).

Immunofluorescence staining of α-Actinin, a cardiac Z-disk protein (Lundy et al., 2013), revealed that the arrangement of sarcomeres in CYC116-treated H1-CMs was more compact and more ordered (Fig. 2A). Sarcomere length was determined in α-Actinin-positive cells as the distance between intensity peaks along the long axis of designated cell area containing clear striations (Ronaldson-Bouchard et al., 2018) (Fig. 2A). Compared to the vehicle group (1.22 ± 0.03 μm), the sarcomere length in the CYC116 group (2.12 ± 0.01 μm, Fig. 2C) was significantly longer and closer to that of adult cardiomyocytes, which is approximately 2.2 μm (Gomez-Garcia et al., 2021). In addition, the size of H1-CMs increased significantly after CYC116 treatment (Figs. 2B and 2D). Immunofluorescent staining also revealed that the adherens junction protein N-cadherin (Supplementary Figs. S2A and S2B) and the gap junction protein connexin 43 (Supplementary Figs. S2C and S2D) were significantly increased in CYC116-treated CMs compared with the control group. The upregulation of these two genes was also confirmed by qRT-PCR analysis (Supplementary Fig. S2E).

The ultrastructure of H1-CMs was characterized by TEM (Fig. 2E). The cardiomyocytes in the control group were relatively immature. The myofibrils were distributed dispersedly in the cytoplasm, lacking the well-organized sarcomeric pattern. In contrast, myofibrils in H1-CMs treated with CYC116 were closely aligned and distributed along a certain direction. In addition, the number of sarcomere structures of individual cardiomyocytes increased compared with the control group. Linear Z-bands that resemble adult CMs could also be observed in H1-CMs treated with CYC116; however, Z-bodies (Zb, fragmented Z-disks) could be observed in H1-CMs treated with DMSO (Fig. 2E). In addition, CYC116-treated H1-CMs had more mitochondria per cell than the control H1-CMs, as determined from the TEM images (Supplementary Fig. S3A, Fig. 2F). In addition, compared with the DMSO treatment group, CYC116-treated H1-CMs showed higher levels of mtDNA (Supplementary Fig. S3B). These data demonstrate that CYC116 promotes the development of myofibrils, the sarcomere structure and junctional proteins, and also increases the number of mitochondria in H1-CMs.

CYC116 increases the ploidy and decreases the proliferative capacity of H1-CMs

During the maturation of cardiomyocytes, their proliferative capacity declines, the cell volume increases, and binuclear or multinuclear cells appear (Ponnusamy et al., 2017). As shown in Fig. 2B, the size of the CMs increased significantly after CYC116 treatment. PI staining also revealed that cells with polyploidy (4c and 8c) were increased significantly after CYC116 treatment, accompanied by a decreased percentage of 2c cells (Figs. 3A and 3B). Ki67 staining was also performed to study the effect of CYC116 on cell proliferation. More than 20% of the H1-CMs generated with the standard protocol were still proliferating, as shown by positive staining for Ki67. In contrast, only 10% of the cells were Ki67 positive after CYC116 treatment, indicating a reduced proliferative capacity and more mature state of cardiomyocytes (Figs. 3C and 3D). In addition, there was a prominent increase in binuclear cells in the CYC116-treated H1-CMs (Fig. 3E), and the multinuclear cells in the CYC116 group were also slightly increased.

CYC116 promotes functional maturation of H1-CMs

Previous studies have shown that the physiological functions of immature hPSC-CMs are different from those of mature cardiomyocytes, including electrophysiological properties, calcium handling and mitochondrial functions. Typically, most reported hPSC-CMs express minimal levels of *KCNJ2* channels, resulting in a less negative resting membrane potential (RMP) at −50 to −60 mv compared to the normal −85 mv in adult cardiomyocytes (Jiang et al., 2018). Here, the AP of H1-CMs was recorded using patch clamp (Figs. 4A and 4B). Most H1-CMs exhibit ventricular-type APs. In CYC116-treated H1-CMs, although the beating frequency and AP duration at 50% (APD50) and 90% (APD90) repolarization did not change significantly compared with the control group, the cells showed a much lower RMP at −82.57 ± 1.87 mV, very close to the value of mature cardiomyocytes. The calcium handling, which is essential for the excitation-contraction coupling of cardiomyocytes (Kolanowski et al., 2017), was also examined. As shown in Figs. 4C and 4D, in CYC116-treated cells, the peak amplitude, upstroke velocity and decay velocity of the calcium signal were all increased significantly compared to those of the control cells. The function of mitochondria is also a critical marker for cardiomyocyte maturation (Feric and Radisic, 2016), so the mitochondrial OCRs were examined (Figs. 4E and 4F). Although there was no significant change in basal and uncoupled respiration, the maximum respiratory rate in the CYC116 group increased significantly. These results confirm that CYC116 treatment promotes the functional maturation of H1-CMs.

Other Aurora kinase inhibitors also promote the maturation of H1-CMs

To verify whether CYC116 promotes H1-CM maturation

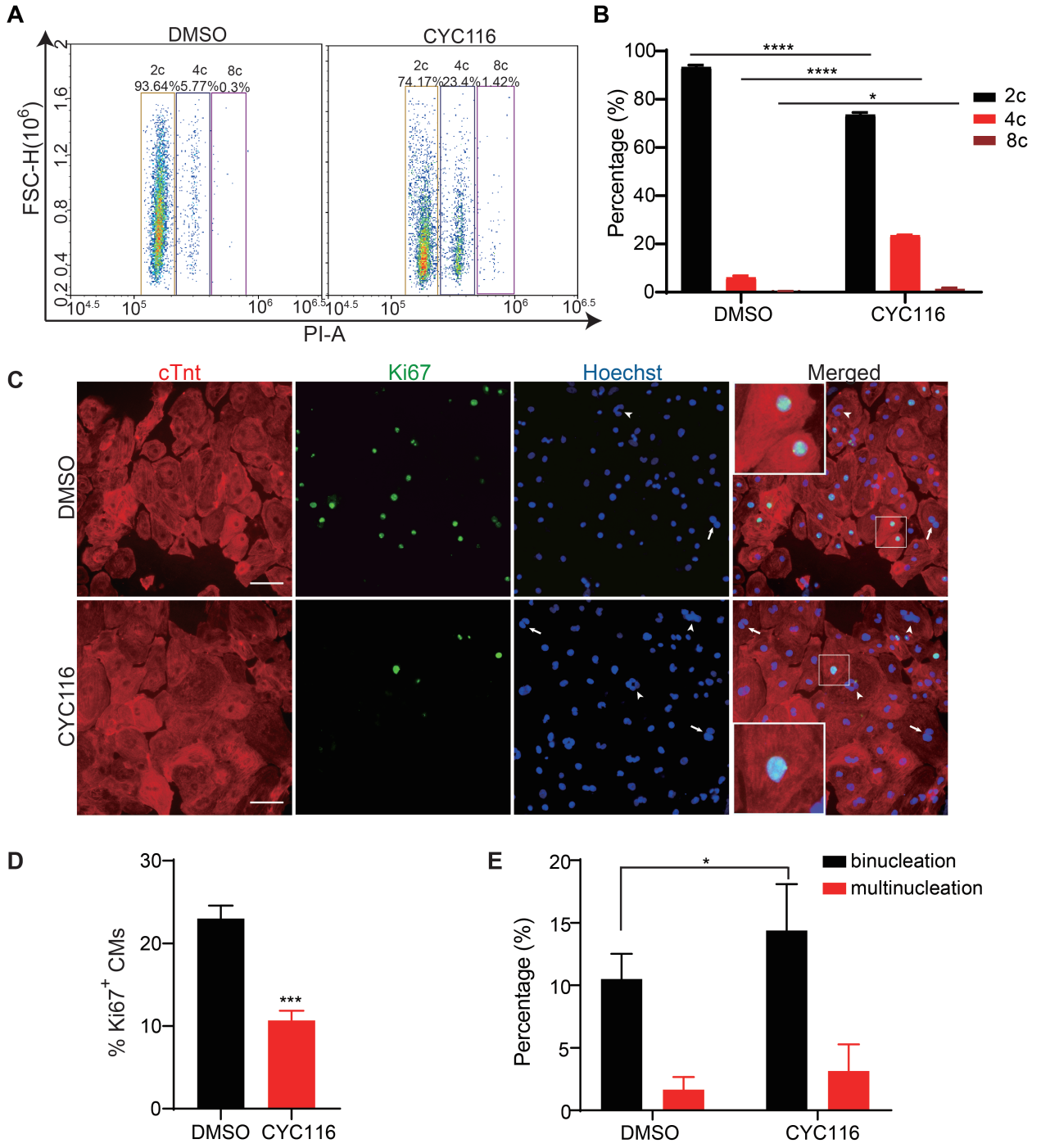

Fig. 3. CYC116 reduces the proliferation of H1-derived cardiomyocytes (H1-CMs). (A and B) Representative flow cytometry image of PI staining (A) and quantitative results of polyploidy ratio in DMSO- and CYC116-treated H1-CMs (B) (n = 3). (C) Representative images of immunofluorescence staining of cTnt and Ki67 in DMSO- or CYC116-treated H1-CMs. The arrows indicate binuclear cells, the arrowheads indicate multinuclear cells. (D and E) The percentage of Ki67-positive cells and the percentage of binuclear and multinuclear cells (Ki67-negative cells) in DMSO- or CYC116-treated H1-CMs (n = 3). Data are presented as the mean ± SEM. $*P < 0.05$; $***P < 0.001$; $****P < 0.0001$.

through Aurora kinase inhibition, we tested a number of other Aurora kinase inhibitors, including the Aurora A and B inhibitors VX-680 (0.5 μM) and SNS-314 (1 μM), the Aurora A inhibitors MLN8237 (0.5 μM) and MK8745 (1 μM), and the Aurora B inhibitors GSK1070916 (0.1 μM) and Barasertib (0.5 μM), using the protocol demonstrated in Fig. 1A. The qRT-PCR results showed that these inhibitors could also promote the expression of genes reflecting mature cardiomyo-

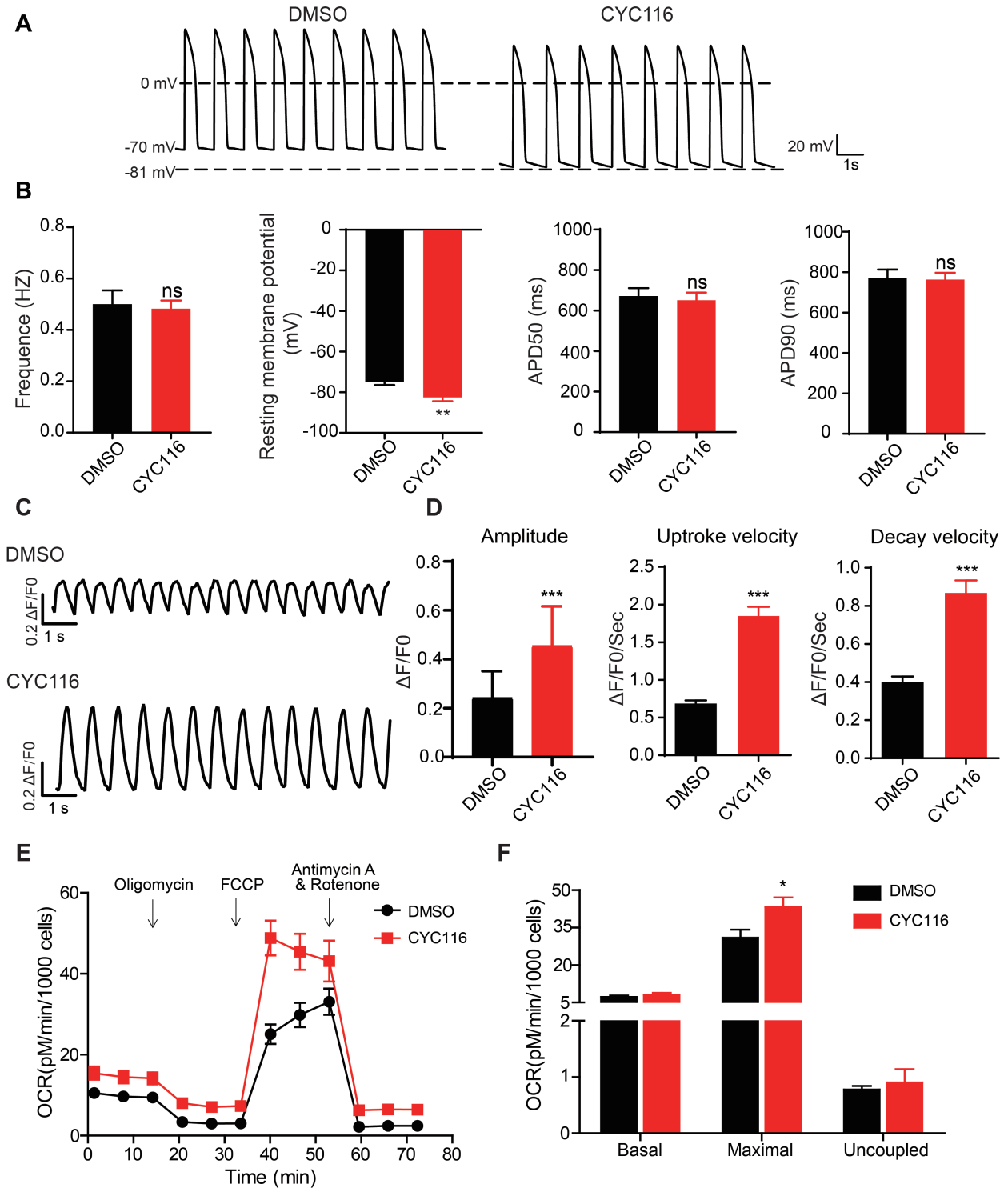

Fig. 4. CYC116 improves functional maturation of H1-derived cardiomyocytes (H1-CMs). (A and B) Representative action potential traces (A) and frequency, resting membrane potential, APD50 and APD90 (B) of H1-CMs treated with DMSO or CYC116 measured by patch clamp (n = 20-30 cells). (C and D) Representative calcium transient (C) and maximum calcium transient amplitude, maximum calcium transient upstroke velocities and maximum calcium transient decay velocities (D) of H1-CMs treated with DMSO or CYC116 (n = 50-70 cells). (E and F) Measurement of mitochondrial respiration levels (E) and statistics for the basal, maximal and uncoupled respiration rates (F) of H1-CMs treated with DMSO or CYC116 (n = 3). Data are presented as the mean ± SEM. $*P < 0.05$; $**P < 0.01$; $***P < 0.001$; ns, not significant.

cyte functions (Supplementary Fig. S4). Therefore, inhibiting Aurora kinase activity might be an effective way to promote cardiomyocyte maturation during *in vitro* differentiation.

CYC116 promotes the maturation of CMs derived from other hPSC cell lines

The above data demonstrate that CYC116 and other Aurora kinase inhibitors may promote the maturation of CMs derived from H1 hESCs. To test whether CYC116 could also promote the maturation of CMs from other hPSCs, we induced the cardiac differentiation of hESC-H9 and hiPSC-UC013 cells (Xue et al., 2013) with the same protocol as that used for hESC-H1 cells (Fig. 1A). On Day 30, similar to H1-CMs, H9-CMs, and UC013-CMs treated with CYC116 showed a certain degree of structural maturity. Immunofluorescence staining and TEM results showed that H9-CMs and UC013-CMs treated with CYC116 had a more orderly sarcomere arrangement (Supplementary Fig. S5A), longer sarcomere length (Fig. 5A) and an increased number of mitochondria per cell (Supplementary Fig. S5B). Calcium transients also showed that H9-CMs and UC013-CMs treated with CYC116 had larger peak amplitudes than the control groups (Fig. 5B).

Transcriptome analysis showed that 2,195 differentially expressed genes were found in H9-CMs treated with CYC116 and DMSO, among which 1,222 genes were upregulated and 973 genes were downregulated. Compared with the control group, genes related to cell structure, contraction function and metabolic function in the CYC116 group were significantly upregulated (Fig. 5C). Furthermore, Gene Ontology (GO) term enrichment analysis showed that the activity of sarcomere structure-related pathways, such as I-band, Z-disc and T-tube, and ion channels, such as voltage-gated channels, were all significantly upregulated in H9-CMs treated with CYC116 (Figs. 5D and 5E).

Ki67-positive H9-CMs and UC013-CMs (Supplementary Fig. S5C) were also decreased significantly in the CYC116 groups compared with the control groups, consistent with the reduced proliferative capacity of mature myocardium. PI

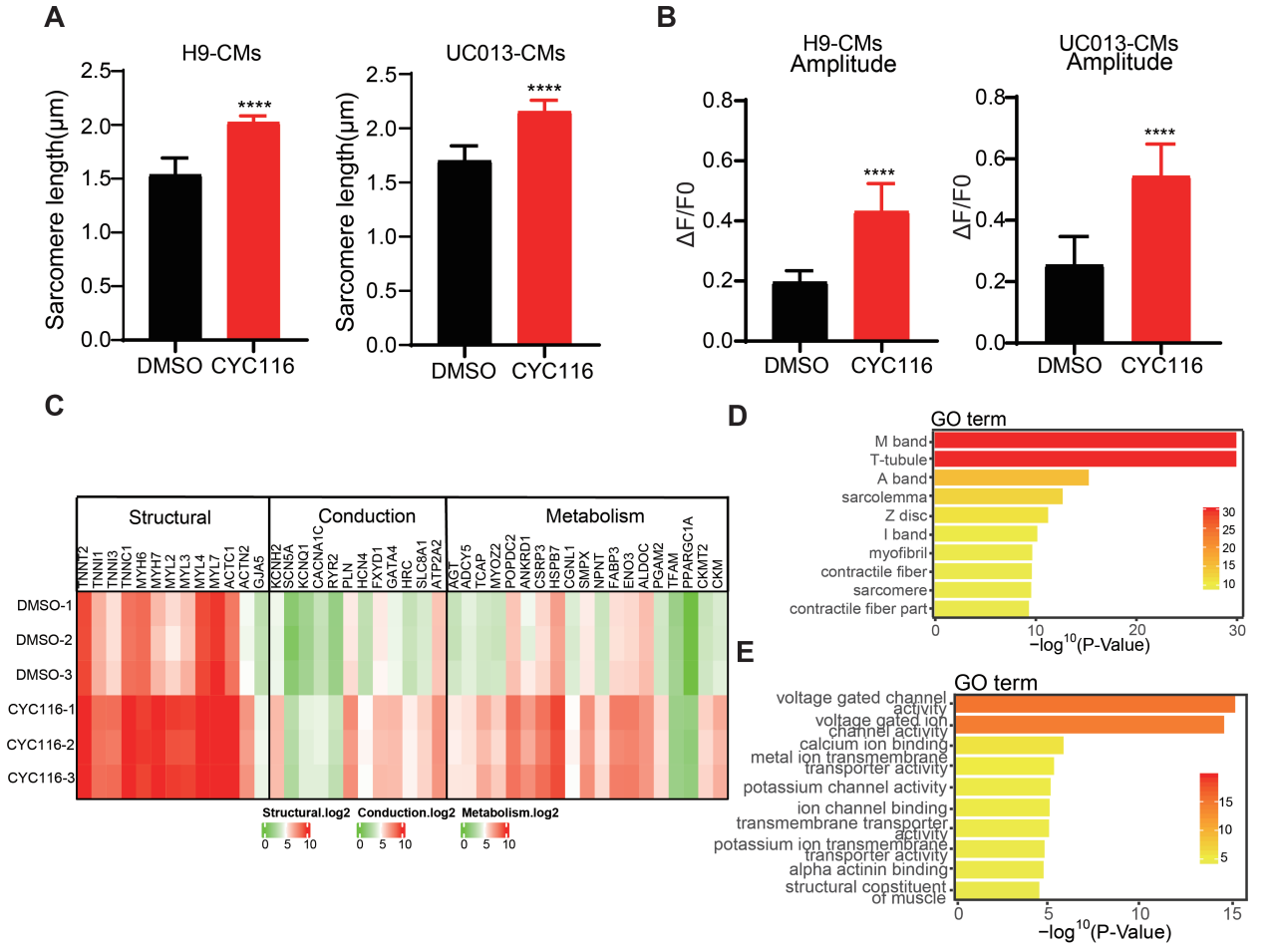

Fig. 5. CYC116 promotes the maturation of cardiomyocytes derived from other hPSCs (human pluripotent stem cell-derived cardiomyocytes). (A) The sarcomere length of CYC116-treated H9-CMs and UC013-CMs (n = 50-80 cells). (B) Maximum calcium transient amplitude of H9-CMs and UC013-CMs treated with DMSO or CYC116 (n = 50-70 cells). Data are presented as mean ± SEM. $^{****}P < 0.0001$. (C) Transcriptome analysis of myocardial specific genes in H9-CMs treated with DMSO or CYC116. (D and E) GO analysis of signaling pathways associated with cardiac structure (D) and ion channels (E) in H9-CMs treated with CYC116 compared with vehicle.

staining and FACS analysis showed that cells with polyploidy (4c and 8c) were increased significantly after CYC116 treatment, accompanied by a decreased percentage of 2c cells (Supplementary Figs. S5D and S5E). These results suggest that CYC116 can also promote the maturation of CMs differentiated *in vitro* from other hPSCs, including hESC-H9 and hiPSC-UC013.

DISCUSSION

In recent years, many efforts have been made to promote the maturation of CMs differentiated *in vitro* from hPSCs. Several laboratories have independently described the characteristics of cardiac maturation in hPSC-CMs or hPSC-derived heart tissues. However, not all methods for promoting myocardial maturation are uniformly scalable, and none can achieve a fully mature phenotype (Gomez-Garcia et al., 2021). Therefore, a continued effort is necessary to identify new scalable ways to generate more mature CMs *in vitro*. Here we discovered that CYC116, an inhibitor of Aurora kinases, significantly promoted the maturation of hPSC-CMs in 2D culture. Aurora kinases are essential kinases that regulate the cell cycle (Borisa and Bhatt, 2017), the role of which has not been studied in hPSC-CM maturation.

Mammalian cardiomyocytes display distinct mechanisms of cell cycle regulation during early development and after birth (Mollova et al., 2013; Porrello et al., 2011). During the developmental period, cardiomyocytes have the ability of DNA synthesis and cytoplasmic division, leading to an increased number of cardiomyocytes (Christoffels et al., 2000). In contrast, postnatal heart growth mainly occurs through the hypertrophic growth of cardiomyocytes. During the perinatal period, cardiomyocytes enter the G1 phase and exit the cell cycle before or after entering the S phase, resulting in an increase in cell size. During this process, some cardiomyocytes shuttle between G and S phases without entering M phase, and the increase in DNA content leads to polyploidy. In addition to polyploidization, some cardiomyocytes can enter the M phase but fail at cytokinesis, resulting in the generation of multinucleation (Ponnusamy et al., 2017). Multinucleation and polyploidy are typical characteristics of adult mammalian cardiomyocytes. Approximately 25% of human cardiomyocytes are binuclear, and 66% of the nuclei are polyploid (Bergmann et al., 2015; Mollova et al., 2013). Considering the natural developmental process, it is hypothesized that the regulation of the cell cycle might be an effective way to promote the maturation of hPSC-CMs during *in vitro* differentiation.

Aurora kinases belong to the serine/threonine kinase family, which controls cell division. There are three members of the Aurora kinases, Aurora A, B and C (Borisa and Bhatt, 2017). Aurora A and B are ubiquitously expressed in many tissues, while Aurora C expression is limited to the testis (Tseng et al., 1998). CYC116 is an effective Aurora A/B inhibitor (Borisa and Bhatt, 2017). Aurora A is located primarily near the centrosomes and spindle poles, driving centrosome maturation, separation, and bipolar spindle assembly (Tang et al., 2017). Aurora B localizes to chromosomes and centromeres in prophase, mediating chromosome condensation. Eventually, it accumulates in the midbody in telophase to phosphorylate microtubule depolymerase, leading to shortening of the central spindle and promoting cytokinesis (Tang et al., 2017). Aurora A/B kinase has been recognized as a key regulator of mitosis, and blocking Aurora A/B activity has been applied in cancer therapy (Yu et al., 2017). Aurora A/B inhibitors have also been reported to increase ploidy and inhibit proliferation in many tumor cells, including human liposarcoma cells, human esophageal squamous cell carcinoma cells, small cell lung cancer cells and breast cancer cells (Du et al., 2019; Noronha et al., 2018; Yu et al., 2017).

Cell cycle regulation may also underlie the maturation promotion effect of previously reported small molecules. The mTOR (mammalian target of rapamycin) signaling inhibitor Torin 1 has been reported to enhance the maturation of hiPSC-CMs by increasing the protein expression of the cell cycle regulator p53, an important mediator directing cellular quiescence (Garbern et al., 2020). T3, a growth hormone essential for optimal heart growth, can significantly increase the size, sarcomere length, and systolic power of cardiomyocytes derived from hPSCs. The effects of T3 are associated with reduced cell cycle activity, for example, reduced DNA synthesis and increased expression of the cyclin-dependent kinase inhibitor P21 (Yang et al., 2014). From these examples and our findings, it is clear that cell cycle change is not only a result of CM maturation but could also be utilized purposfully to promote CM maturation *in vitro*.

Here, we found that inhibiting Aurora kinases with CYC116 or other inhibitors significantly promoted the maturation of CMs derived from both hESCs (H1 and H9) and iPSCs (UC013), resulting in increased expression of genes related to cardiomyocyte function, better organization of the sarcomere, increased sarcomere length, increased number of mitochondria, and enhanced physiological function of the cells. These results suggest that regulating the cell cycle might be an effective way to promote CM maturation *in vitro*.

Note: Supplementary information is available on the Molecules and Cells website (www.molcells.org).

ACKNOWLEDGMENTS
This work was supported by grants from the Chinese Academy of Sciences (XDA16010202), the Ministry of Science and Technology of China (2017YFA0104002), and the National Natural Science Foundation of China (82121005, 81730099).

AUTHOR CONTRIBUTIONS
S.J. performed most of the experiments, analyzed the data, prepared the figures and drafted the manuscript. W.T., C.H., Z.C., X.R., and B.H. participated in some of the experiments, X.D. and Y.C. provided critical materials, X.X. conceived the idea, supervised the study, analyzed the data and edited the manuscript.

CONFLICT OF INTEREST
The authors have no potential conflicts of interest to disclose.

ORCID
Sijia Ji https://orcid.org/0000-0001-8181-5137

Wanzhi Tu https://orcid.org/0000-0003-3169-6250
Chenwen Huang https://orcid.org/0000-0002-9099-6715
Ziyang Chen https://orcid.org/0000-0003-2270-9558
Xinyue Ren https://orcid.org/0000-0003-3632-7155
Bingqing He https://orcid.org/0000-0003-4928-5601
Xiaoyan Ding https://orcid.org/0000-0003-4698-4829
Yuelei Chen https://orcid.org/0000-0002-2200-6652
Xin Xie https://orcid.org/0000-0003-2314-4800

REFERENCES

Angst, B.D., Khan, L.U., Severs, N.J., Whitely, K., Rothery, S., Thompson, R.P., Magee, A.I., and Gourdie, R.G. (1997). Dissociated spatial patterning of gap junctions and cell adhesion junctions during postnatal differentiation of ventricular myocardium. Circ. Res. *80*, 88-94.

Barth, E., Stämmler, G., Speiser, B., and Schaper, J. (1992). Ultrastructural quantitation of mitochondria and myofilaments in cardiac muscle from 10 different animal species including man. J. Mol. Cell. Cardiol. *24*, 669-681.

Bergmann, O., Zdunek, S., Felker, A., Salehpour, M., Alkass, K., Bernard, S., Sjostrom, S.L., Szewczykowska, M., Jackowska, T., Dos Remedios, C., et al. (2015). Dynamics of cell generation and turnover in the human heart. Cell *161*, 1566-1575.

Bhattacharya, S., Burridge, P.W., Kropp, E.M., Chuppa, S.L., Kwok, W.M., Wu, J.C., Boheler, K.R., and Gundry, R.L. (2014). High efficiency differentiation of human pluripotent stem cells to cardiomyocytes and characterization by flow cytometry. J. Vis. Exp. *91*, 52010.

Borisa, A.C. and Bhatt, H.G. (2017). A comprehensive review on Aurora kinase: small molecule inhibitors and clinical trial studies. Eur. J. Med. Chem. *140*, 1-19.

Burridge, P.W., Matsa, E., Shukla, P., Lin, Z.C., Churko, J.M., Ebert, A.D., Lan, F., Diecke, S., Huber, B., Mordwinkin, N.M., et al. (2014). Chemically defined generation of human cardiomyocytes. Nat. Methods *11*, 855-860.

Cao, F., Wagner, R.A., Wilson, K.D., Xie, X., Fu, J.D., Drukker, M., Lee, A., Li, R.A., Gambhir, S.S., Weissman, I.L., et al. (2008). Transcriptional and functional profiling of Human pluripotent stem cell-derived cardiomyocytes. PLoS One *3*, e3474.

Christoffels, V.M., Habets, P.E., Franco, D., Campione, M., de Jong, F., Lamers, W.H., Bao, Z.Z., Palmer, S., Biben, C., Harvey, R.P., et al. (2000). Chamber formation and morphogenesis in the developing mammalian heart. Dev. Biol. *223*, 266-278.

Du, J., Yan, L., Torres, R., Gong, X., Bian, H., Marugán, C., Boehnke, K., Baquero, C., Hui, Y.H., Chapman, S.C., et al. (2019). Aurora A–selective inhibitor LY3295668 leads to dominant mitotic arrest, apoptosis in cancer cells, and shows potent preclinical antitumor efficacy. Mol. Cancer Ther. *18*, 2207-2219.

Feric, N.T. and Radisic, M. (2016). Maturing human pluripotent stem cell-derived cardiomyocytes in human engineered cardiac tissues. Adv. Drug Deliv. Rev. *96*, 110-134.

Garbern, J.C., Helman, A., Sereda, R., Sarikhani, M., Ahmed, A., Escalante, G.O., Ogurlu, R., Kim, S.L., Zimmerman, J.F., Cho, A., et al. (2020). Inhibition of mTOR signaling enhances maturation of cardiomyocytes derived from human-induced pluripotent stem cells via p53-induced quiescence. Circulation *141*, 285-300.

Goffart, S., von Kleist-Retzow, J.C., and Wiesner, R.J. (2004). Regulation of mitochondrial proliferation in the heart: power-plant failure contributes to cardiac failure in hypertrophy. Cardiovasc. Res. *64*, 198-207.

Gomez-Garcia, M.J., Quesnel, E., Al-Attar, R., Laskary, A.R., and Laflamme, M.A. (2021). Maturation of human pluripotent stem cell derived cardiomyocytes in vitro and in vivo. Semin. Cell Dev. Biol. *118*, 163-171.

Hu, D., Linders, A., Yamak, A., Correia, C., Kijlstra, J.D., Garakani, A., Xiao, L., Milan, D.J., van der Meer, P., Serra, M., et al. (2018). Metabolic maturation of human pluripotent stem cell-derived cardiomyocytes by inhibition of HIF1alpha and LDHA. Circ. Res. *123*, 1066-1079.

Jiang, Y., Park, P., Hong, S.M., and Ban, K. (2018). Maturation of cardiomyocytes derived from human pluripotent stem cells: current strategies and limitations. Mol. Cells *41*, 613-621.

Kadota, S., Pabon, L., Reinecke, H., and Murry, C.E. (2017). In vivo maturation of human induced pluripotent stem cell-derived cardiomyocytes in neonatal and adult rat hearts. Stem Cell Reports *8*, 278-289.

Kamakura, T., Makiyama, T., Sasaki, K., Yoshida, Y., Wuriyanghai, Y., Chen, J., Hattori, T., Ohno, S., Kita, T., Horie, M., et al. (2013). Ultrastructural maturation of human-induced pluripotent stem cell-derived cardiomyocytes in a long-term culture. Circ. J. *77*, 1307-1314.

Kolanowski, T.J., Antos, C.L., and Guan, K. (2017). Making human cardiomyocytes up to date: derivation, maturation state and perspectives. Int. J. Cardiol. *241*, 379-386.

Liang, P., Lan, F., Lee, A.S., Gong, T., Sanchez-Freire, V., Wang, Y., Diecke, S., Sallam, K., Knowles, J.W., Wang, P.J., et al. (2013). Drug screening using a library of human induced pluripotent stem cell-derived cardiomyocytes reveals disease-specific patterns of cardiotoxicity. Circulation *127*, 1677-1691.

Liu, Y., Bai, H., Guo, F., Thai, P.N., Luo, X., Zhang, P., Yang, C., Feng, X., Zhu, D., Guo, J., et al. (2020). PPARGC1A activator ZLN005 promotes maturation of cardiomyocytes derived fromHuman pluripotent stem cells. Aging (Albany N.Y.) *12*, 7411-7430.

Lundy, S.D., Zhu, W.Z., Regnier, M., and Laflamme, M.A. (2013). Structural and functional maturation of cardiomyocytes derived from human pluripotent stem cells. Stem Cells Dev. *22*, 1991-2002.

Miao, S., Zhao, D., Wang, X., Ni, X., Fang, X., Yu, M., Ye, L., Yang, J., Wu, H., Han, X., et al. (2020). Retinoic acid promotes metabolic maturation of human embryonic stem cell-derived cardiomyocytes. Theranostics *10*, 9686-9701.

Mills, R.J., Titmarsh, D.M., Koenig, X., Parker, B.L., Ryall, J.G., Quaife-Ryan, G.A., Voges, H.K., Hodson, M.P., Ferguson, C., Drowley, L., et al. (2017). Functional screening in human cardiac organoids reveals a metabolic mechanism for cardiomyocyte cell cycle arrest. Proc. Natl. Acad. Sci. U. S. A. *114*, E8372-E8381.

Mollova, M., Bersell, K., Walsh, S., Savla, J., Das, L.T., Park, S.Y., Silberstein, L.E., Dos Remedios, C.G., Graham, D., Colan, S., et al. (2013). Cardiomyocyte proliferation contributes to heart growth in young humans. Proc. Natl. Acad. Sci. U. S. A. *110*, 1446-1451.

Moretti, A., Bellin, M., Welling, A., Jung, C.B., Lam, J.T., Bott-Flügel, L., Dorn, T., Goedel, A., Höhnke, C., Hofmann, F., et al. (2010). Patient-specific induced pluripotent stem-cell models for long-QT syndrome. N. Engl. J. Med. *363*, 1397-1409.

Noronha, S., Alt, L.A.C., Scimeca, T.E., Zarou, O., Obrzut, J., Zanotti, B., Hayward, E.A., Pillai, A., Mathur, S., Rojas, J., et al. (2018). Preclinical evaluation of the Aurora kinase inhibitors AMG 900, AZD1152-HQPA, and MK-5108 on SW-872 and 93T449 human liposarcoma cells. In Vitro Cell. Dev. Biol. Anim. *54*, 71-84.

Parikh, S.S., Blackwell, D.J., Gomez-Hurtado, N., Frisk, M., Wang, L., Kim, K., Dahl, C.P., Fiane, A., Tønnessen, T., Kryshtal, D.O., et al. (2017). Thyroid and glucocorticoid hormones promote functional T-tubule development in human-induced pluripotent stem cell-derived cardiomyocytes. Circ. Res. *121*, 1323-1330.

Ponnusamy, M., Li, P.F., and Wang, K. (2017). Understanding cardiomyocyte proliferation: an insight into cell cycle activity. Cell. Mol. Life Sci. *74*, 1019-1034.

Porrello, E.R., Mahmoud, A.I., Simpson, E., Hill, J.A., Richardson, J.A., Olson, E.N., and Sadek, H.A. (2011). Transient regenerative potential of the neonatal mouse heart. Science *331*, 1078-1080.

Robertson, C., Tran, D.D., and George, S.C. (2013). Concise review:

maturation phases of human pluripotent stem cell-derived cardiomyocytes. Stem Cells *31*, 829-837.

Rog-Zielinska, E.A., Craig, M.A., Manning, J.R., Richardson, R.V., Gowans, G.J., Dunbar, D.R., Gharbi, K., Kenyon, C.J., Holmes, M.C., Hardie, D.G., et al. (2015). Glucocorticoids promote structural and functional maturation of foetal cardiomyocytes: a role for PGC-1alpha. Cell Death Differ. *22*, 1106-1116.

Ronaldson-Bouchard, K., Ma, S.P., Yeager, K., Chen, T., Song, L., Sirabella, D., Morikawa, K., Teles, D., Yazawa, M., and Vunjak-Novakovic, G. (2018). Advanced maturation of human cardiac tissue grown from pluripotent stem cells. Nature *556*, 239-243.

Tang, A., Gao, K., Chu, L., Zhang, R., Yang, J., and Zheng, J. (2017). Aurora kinases: novel therapy targets in cancers. Oncotarget *8*, 23937-23954.

Tertoolen, L.G.J., Braam, S.R., van Meer, B.J., Passier, R., and Mummery, C.L. (2018). Interpretation of field potentials measured on a multi electrode array in pharmacological toxicity screening on primary and human pluripotent stem cell-derived cardiomyocytes. Biochem. Biophys. Res. Commun. *497*, 1135-1141.

Tseng, T.C., Chen, S.H., Hsu, Y.P., and Tang, T.K. (1998). Protein kinase profile of sperm and eggs: cloning and characterization of two novel testis-specific protein kinases (AIE1, AIE2) related to yeast and fly chromosome segregation regulators. DNA Cell Biol. *17*, 823-833.

Xu, X.Q., Soo, S.Y., Sun, W., and Zweigerdt, R. (2009). Global expression profile of highly enriched cardiomyocytes derived from Human pluripotent stem cells. Stem Cells *27*, 2163-2174.

Xue, Y., Cai, X., Wang, L., Liao, B., Zhang, H., Shan, Y., Chen, Q., Zhou, T., Li, X., Hou, J., et al. (2013). Generating a non-integrating human induced pluripotent stem cell bank from urine-derived cells. PLoS One *8*, e70573.

Yang, X., Pabon, L., and Murry, C.E. (2014). Engineering adolescence: maturation of human pluripotent stem cell-derived cardiomyocytes. Circ. Res. *114*, 511-523.

Yang, X., Rodriguez, M., Pabon, L., Fischer, K.A., Reinecke, H., Regnier, M., Sniadecki, N.J., Ruohola-Baker, H., and Murry, C.E. (2014). Tri-iodo-l-thyronine promotes the maturation of human cardiomyocytes-derived from induced pluripotent stem cells. J. Mol. Cell. Cardiol. *72*, 296-304.

Yang, X., Rodriguez, M.L., Leonard, A., Sun, L., Fischer, K.A., Wang, Y., Ritterhoff, J., Zhao, L., Kolwicz, S.C., Jr., Pabon, L., et al. (2019). Fatty acids enhance the maturation of cardiomyocytes derived from human pluripotent stem cells. Stem Cell Reports *13*, 657-668.

Yu, X., Liang, Q., Liu, W., Zhou, L., Li, W., and Liu, H. (2017). Deguelin, an Aurora B kinase inhibitor, exhibits potent anti-tumor effect in human esophageal squamous cell carcinoma. EBioMedicine *26*, 100-111.